23p.

PRELIMINARY DATA

RESULTS ON GAMMA-RAY ASTRONOMY FROM EXPLORER XI*

by

G. W. Clark and W. L. Kraushaar
Massachusetts Institute of Technology
Cambridge, Massachusetts

Explorer XI was launched on April 27, 1961. It carried a single experiment whose purpose was to make astronomical observations with high energy primary cosmic gamma rays. The gamma ray detector was prepared at MIT with the aid of Mr. Gordon Garmire and other members of our laboratory. The spacecraft and rocket were the responsibility of the George Marshall Space Flight Center. The data were acquired and sent to us by the Goddard Space Flight Center and the entire project was coordinated by Dr. James Kupperian for the National Aeronautics and Space Administration.

Before describing the experiment and the results we have obtained from it so far, we consider first what expectations one might have for high energy gamma ray astronomy.

First of all, we restrict the term "high energy gamma rays" to that portion of the electromagnetic spectrum where the predominate process for the interaction of photons with matter is the production of electron pairs. An electron pair tends to proceed in the direction of the incident photon, and so an appropriately arranged counter telescope can perform as a directional detector of high energy gamma rays - in effect as a gamma ray telescope.

* This work was supported primarily by funds provided by the National Aeronautics and Space Administration, and partly by funds from the U. S. Atomic Energy Commission, Office of Naval Research, and Air Force Office of Scientific Research.

As a result the practical problems of high energy gamma ray astronomy are rather different from those encountered at the lower energies which are typical of nuclear energy levels. The gamma ray telescope in Explorer XI was sensitive, specifically, above about 50 Mev.

Any cosmic radiation that comes to us without interference straight from its source has a directional intensity at the earth which is the line integral of its source strength per unit solid angle along the line of sight. Of course this is not the case with the charged particles that constitute the ordinary cosmic rays. Their trajectories are twisted by the general galactic magnetic field into helices whose radii are generally very small in comparison to galactic dimensions. Thus whatever may be the source distribution and strength for charged cosmic rays, the local observed cosmic ray intensity is highly isotropic because of magnetic stirring, and it has a magnitude that depends not only on the source strength, but also on the effectiveness with which the magnetic field prevents escape from the galaxy.

The simple relation between source strength and observed directional intensity also does not hold for visible light which can be totally absorbed or scattered by the interstellar dust. Indeed, our view in directions that lie in the galactic plane is blocked by cosmic dust clouds in many directions at distances that amount to only small fractions of a galactic diameter. In these directions the sky looks black in spite of the countless stellar sources of visible light that must lie beyond the dust clouds.

The simple relation between source strength and observed intensity does hold, however, for magnetic brehmsstrahlung radio waves and gamma rays. Both can traverse a galactic diameter without significant attenuation. Moreover their source strengths depend on physical conditions that are closely related to one another.

It appears that the most important source of cosmic gamma rays is nuclear interactions of ordinary charged cosmic ray protons with interstellar gas protons. These interactions produce both charged and neutral pi mesons which are unstable and quickly decay. The charged mesons give most of their energy to electrons which then spiral in the galactic magnetic field and gradually radiate their energies at radio frequencies by the process of magnetic brehmsstralung or synchrotron radiation. The neutral pi mesons, on the other hand, decay into gamma rays which fly directly away from the point of interaction. At first sight, therefore, one might expect the source strengths for radio emission and gamma rays to be the same and the patterns of the so-called isophotes of radio and gamma radiation to be identical. But the situation is certainly more complicated than this. First of all, in the time it takes for an electron to radiate its energy as radio waves it can travel over distances comparable to the dimensions of the galaxy. Thus even if electrons gain most of their energy in the galactic disc, or even in supernovae, they can escape into the halo and give radio emission at large galactic latitudes as is indeed, observed. Another reason why there may not be a close identity between gamma and radio emission is that cosmic electrons may have their energy not only by being born rich with it, but also through gradual acceleration in galactic space or possibly within the shells of supernovae.

However, since the production of gamma rays in nuclear interactions is necessarily accompanied by the production of electrons, the total synchrotron radio power generated in the galaxy can hardly be less than the gamma ray power. And the directional distribution of gamma rays will give us directly the spatial distribution of the nuclear interactions which are the ultimate source of at least a portion of the radio power.

When gamma ray observations are refined and angular resolution is improved, it should be possible to measure the rate of high energy nuclear interactions in individual supernova shells like the Crab Nebula. Here too, a comparison of the radio and gamma ray power output will tell us much about the relative importance of Fermi accleration and nuclear interactions in giving energy to the cosmic electrons.

With these ideas in mind we can make order of magnitude estimates of the expected intensity of cosmic gamma rays. We look first directly at the interaction of cosmic rays with interstellar matter in the galactic disc, and find the source strength per unit solid angle by multiplying together the cosmic ray intensity, the matter density, the cross section and the average multiplicity for gamma ray production in a nuclear interaction. This source strength, 2.4×10^{-26} cm^{-3} sec^{-1} st^{-1}, when multiplied by the average distance to the boundary of the disc, 5×10^{21} cm, gives a predicted intensity of about 10^{-4} cm^{-2} sec^{-1} st^{-1}. This amounts to about one in three thousand ordinary cosmic rays.

For a second estimate we use the idea that the total galactic radio power incident on the earth must equal or exceed the galactic gamma ray power. We can therefore calculate an upper limit for the gamma ray intensity by dividing the observed radio power by the average quantum energy of gamma rays from π^0 decay which we take to be 200 Mev. Using values for radio emission given by Ginsburg[1] we find a gamma ray intensity of 3×10^{-4} cm^{-2} sec^{-1} st^{-1}.

The similarity of these two values reflects the fact that one can actually come close to explaining radio emission entirely in terms of charged pi mesons production.

The large ratios between the ordinary cosmic ray intensity and the expected gamma ray intensity define the essential practical problem of gamma ray astronomy which is how to distinguish the rare gamma rays in the midst of the far more abundant charged cosmic rays. In Explorer XI this was done with a directional counter telescope that was surrounded by a very efficient anticoincidence shield or veto counter. The arrangement is shown in Figure 1. A gamma ray interacts in the high Z sandwich scintillator, and the resultant electron pair passes through the directional Cerenkov detector. The signature of a gamma ray is therefore taken to be coincident pulses from the scintillator and the Cerenkov detector with no pulse from the veto counter. When this happened during regular operation, the height of the pulse from the scintillator was telemetered. Now and then, on command from the ground, the veto counter was turned off so that events due to energetic charged particles were recorded at a high rate for calibration purposes. In addition, a scaling circuit could be connected on command to any one of several positions in the circuit so that the performance of the detectors as well as the simple coincidence rate between the scintillator and Cerenkov detector could be monitored.

The complete satellite went into orbit spinning about its long axis which was in fact the axis of the telescope. It remained in this state for about twenty days, and during this first phase the viewing direction of the telescope slowly scanned across the sky at a rate of about 10° per day as the angular momentum changed under the influence of very small torques. During every orbit the earth's disc moved across the field of view from horizon to horizon, and forward-looking, narrow angle optical sensors enable us to identify the instants of the horizon crossings. Near the end of the first twenty days the satellite motion suddenly changed, as planned, into a tumble about an axis perpendicular to its long direction. In this second phase the satellite tumbled with a period of about 13 seconds, and the direction of viewing scanned a great circle around the sky which generally included a sweep of the earth from horizon to horizon.

Throughout the experiment it was essential to keep exact account of when the telescope was viewing the earth because the intensity of albedo gamma rays far exceeds that of cosmic gamma rays. Furthermore, to derive a value for the intensity of cosmic gamma rays it is necessary to keep careful account of the exposure times in various parts of the sky.

The telescope itself apparently performed in orbit essentially as planned for about five months. However, the data could be received only when the satellite was over one of the Minitrack stations which was about 20% of the total time. Only 30% of this time was useful because the rest was spent in the Van Allen radiation which jammed the detectors. And during about 50% of the remaining time the telescope was viewing the earth. Thus all together only about 3% of the orbit time during five months was useful observing time, which explains the paucity of data we can present. Needless to say, these specific difficulties are not inherent in satellite gamma ray astronomy, and can be eliminated in future experiments.

Now as to the performance of the detector. First of all there seems to be no doubt that the instrument was selectively sensitive to high energy gamma rays. This was established by tests at the MIT synchrotron as well as by its performance in the natural radiation.

The synchrotron tests showed that the instrument responded to gamma rays with an aperture cone of about 17° half angle.

The altitude variation of the gamma ray counting rate measured during a balloon test is shown in Figure 2. Note the high altitude decrease in the gamma ray rate. This indicates their secondary character. Incidentally, the rate in orbit was two decades below the last point shown here and this illustrates the necessity of using a satellite to carry the telescope above the atmosphere. Indeed the production of gamma rays in the atmosphere by primary cosmic rays is entirely analogous to their production in interstellar space except that the target nuclei are oxygen and nitrogen instead of hydrogen. In fact, the counting rate under the known atmospheric thickness has provided a good check on the interpretation of the counting rates observed in orbit.

In orbit the effect of the atmosphere in producing albedo gamma rays can be clearly seen. Figure 3 shows some of the gamma ray events recorded during the first spin phase as a function of time reduced modulo the orbital period. Each line represents the history of one orbit, and in this plot the horizon crossings of which there are two per orbit, occur at nearly the same place on successive orbits. The listening station seems to move past underneath the orbit as the earth turns. Clearly the rate of gamma ray events drops off sharply as the horizon is crossed. In fact the ratio of the average rate of albedo to the cosmic rate is about 10 to 1. In sharp contrast, the rates of charged particles during calibration orbits show the opposite effect, as expected, being greater from the sky than from the earth.

Figure 4 shows the albedo effect observed during the tumble phase when a more elaborate analysis is required to keep track of the orientation. These albedo observations are proof that the telescope was selectively sensitive to gamma rays in orbit. Furthermore the measured intensity of albedo gamma rays is consistent with earlier balloon observations.

The remaining critical question is whether the so-called gamma ray events observed from the sky were gamma rays or some obscure form of background. The pulse height distributions obtained during calibration and with gamma ray logic are shown in Figure 5. As one would expect, during calibration a considerable fraction of the pulses are saturated from the effects of nuclear interactions and heavy primaries. Such saturated pulses are totally absent from the events registered with gamma ray logic. If all the so-called gamma ray events were really protons that somehow managed to slip through the veto counter shield, we should have seen six large pulses due to nuclear interactions. We conclude, therefore, that veto counter inefficiency is not a significant source of background. Another and probably more dangerous source of background is the decay of unstable particles, particularly mu mesons, that stop in the sandwich scintillator and decay after the veto counter circuitry has recovered from the passage of the incident producing particle. The magnitude of this effect is difficult to evaluate accurately. We feel it could account for 25% of our observed apparent "gamma ray" rate.

Conclusive evidence that the 64 events we have reported were really cosmic gamma rays would, of course, be provided by an observed anisotropy. Unfortunately, when the few events we have are spread out on a celestial map it is not possible to draw any definite conclusion regarding their distribution. Figure 6 shows the arrival direction of each event, without any accounting for exposure time. The dotted line indicates the trail of the satellite angular momentum across the sky in the first spin phase.

Figure 7 shows the areas in which the observed number of events exceeded the expected number assuming perfect isotropy and taking account of exposure times. One cannot see a striking anisotropy in the observed intensity, which would establish beyond doubt that the observed events were indeed gamma rays. On the other hand these data are few and future observations may bring out such an anisotropy. Lacking an observed anisotropy, we must regard our measured intensities as upper limits.

During the tumble phase nearly the whole sky was scanned at one time or another although the exposure was quite uneven. 55 events were recorded during 1.3 days of effective observing time. Taking into account the geometrical factor and the detection efficiency we arrive at an average intensity which lies between 3 and 10×10^{-4} cm^{-2} sec^{-1} st^{-1}. This result is somewhat greater than the expected values we gave before, but clearly not in serious disagreement in view of the uncertainties in the values that were used. The result is consistent, however, with the idea that most of the energy radiated by cosmic electrons is given to them at their birth in nuclear interactions.

Upper limits to the intensities from objects of special interest like the Crab Nebula can also be obtained from our data. Now and then, as the angular momentum wandered through the sky, the satellite would, for a period of a day or so, repeatedly scan past one of these objects. Occasionally a gamma ray event would be recorded when the object was somewhere within the cone of resolution. In this case we attributed to the object a fraction of the event depending on how close it was to the center of the cone. Similarly, we attributed an effective exposure time for each scan depending on how close to the center of the cone passed. The results are summarized in Table I.

TABLE I

Predicted galactic contribution from cosmic ray - gas collision processes	$J \quad 10^{-4} cm^{-2} sec^{-1} sr^{-1}$
Measured upper limit of apparent isotropic component	$J^{I} < 3 - 10 \times 10^{-4} cm^{-2} sec^{-1} sr^{-1}$

Upper limits to the flux from various possible sources

Cassiopeia A	$< 4.8 \times 10^{-4} cm^{-2} sec^{-1}$
Andromeda	< 5.5
Cygnus A	< 3.6
Taurus A (Crab)	< 18.4
Galactic Center	< 6.2
Sun	< 13.6

FIGURE CAPTION

Figure 1. The gamma ray detector.

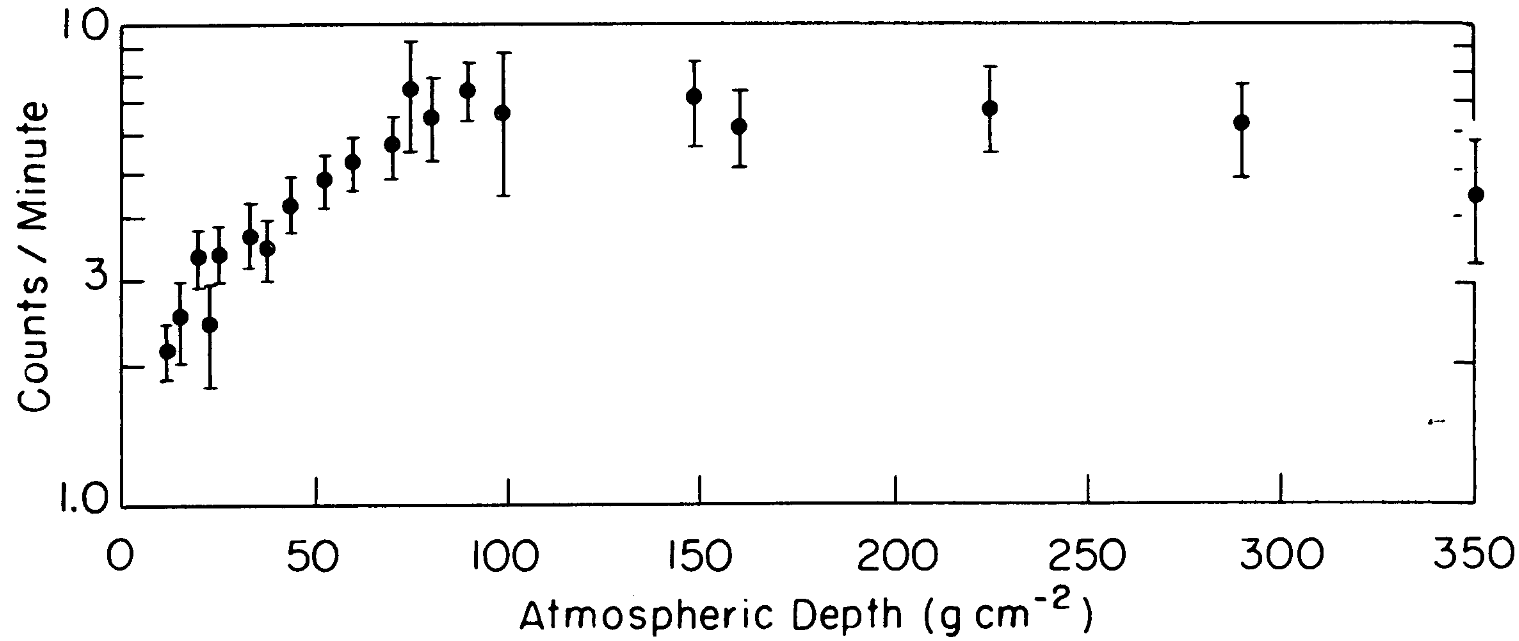

Counts / Minute
10
3
1.0
0
50
100
150
200
250
300
350
Atmospheric Depth (g cm^{-2})

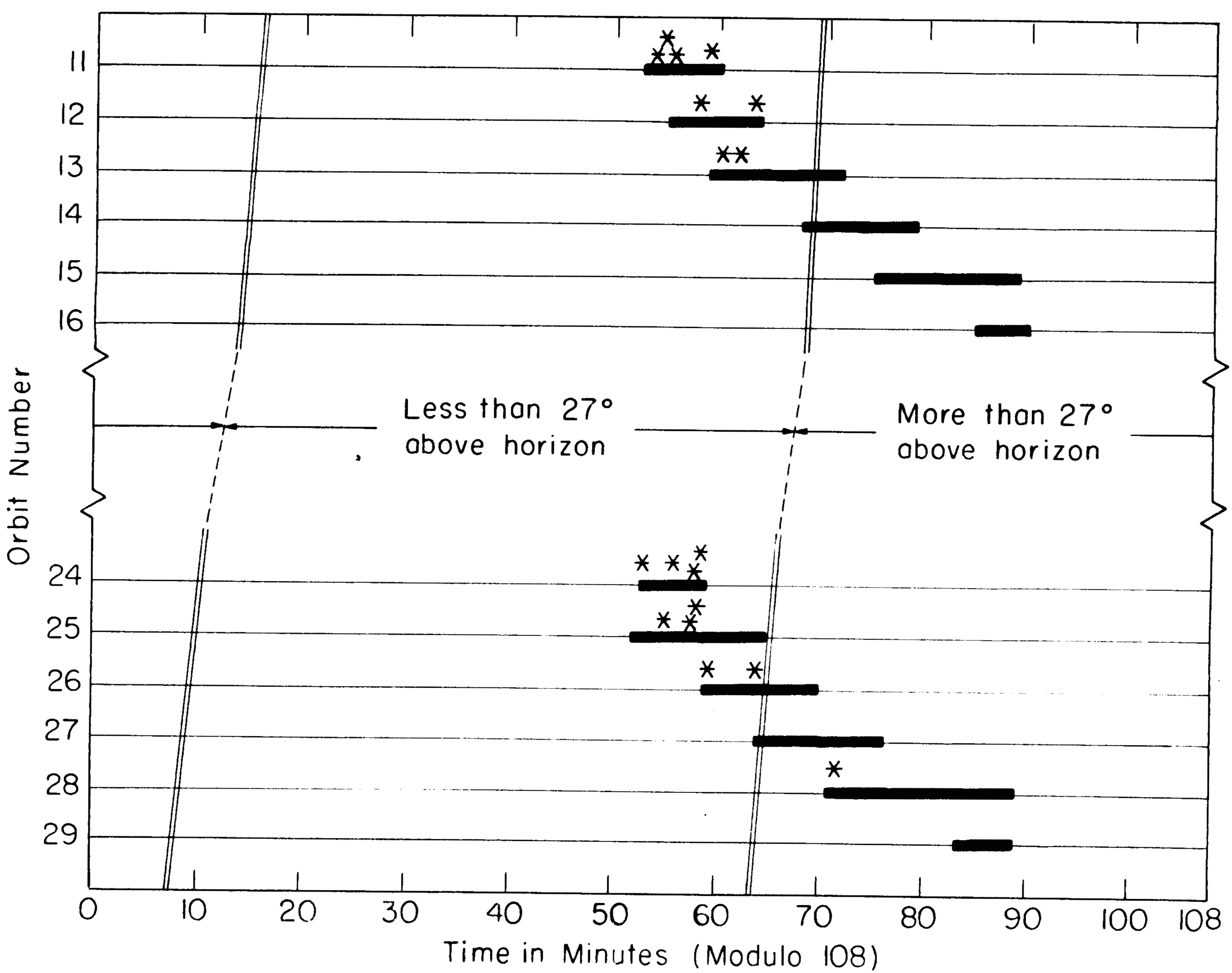

Orbit Number
11
12
13
14
15
16
24
25
26
27
28
29
Less than 27°
above horizon
More than 27°
above horizon
0
10
20
30
40
50
60
70
80
90
100
108
Time in Minutes (Modulo 108)

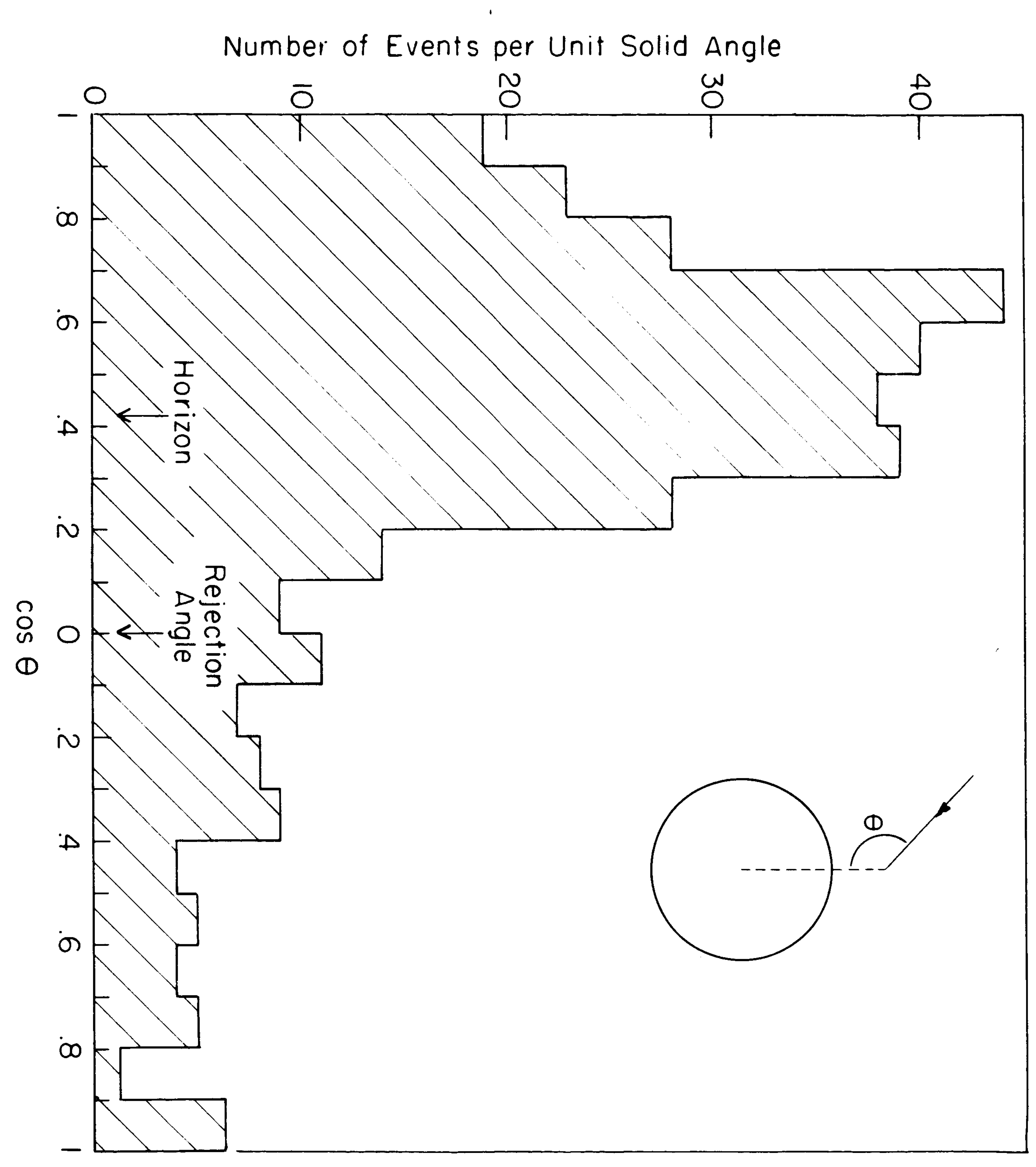
Number of Events per Unit Solid Angle
0
10
20
30
40
1
.8
.6
.4
.2
0
.2
.4
.6
.8
1
cos θ
Horizon
Rejection Angle
θ

[redacted]

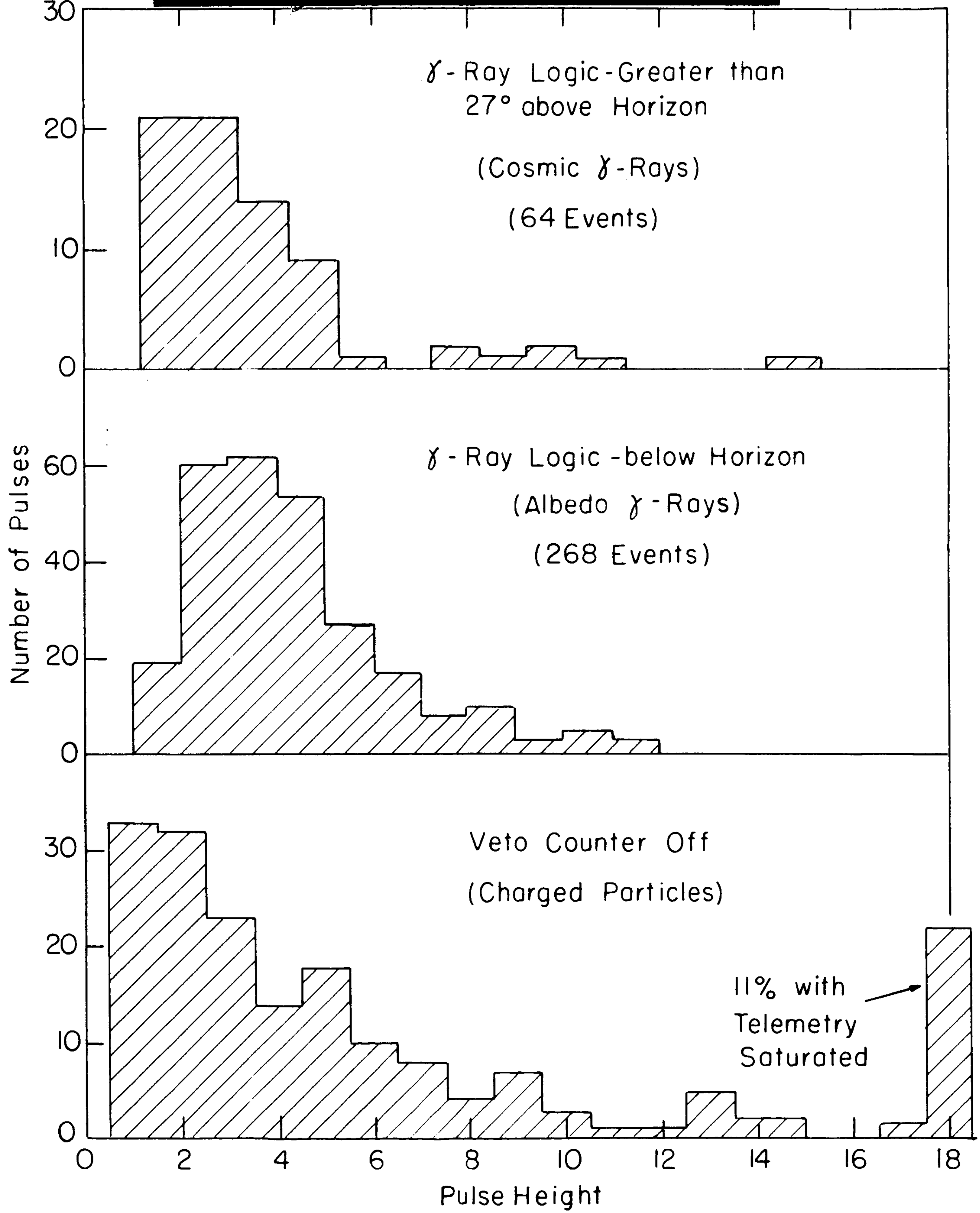

γ - Ray Logic - Greater than 27° above Horizon
(Cosmic γ - Rays)
(64 Events)
γ - Ray Logic - below Horizon
(Albedo γ - Rays)
(268 Events)
Veto Counter Off
(Charged Particles)
11% with Telemetry Saturated
Number of Pulses
Pulse Height
30
20
10
0
60
40
20
0
30
20
10
0
0
2
4
6
8
10
12
14
16
18

GAMMA RAY EVENTS PLOTTED
ON EQUAL AREA PROJECTION

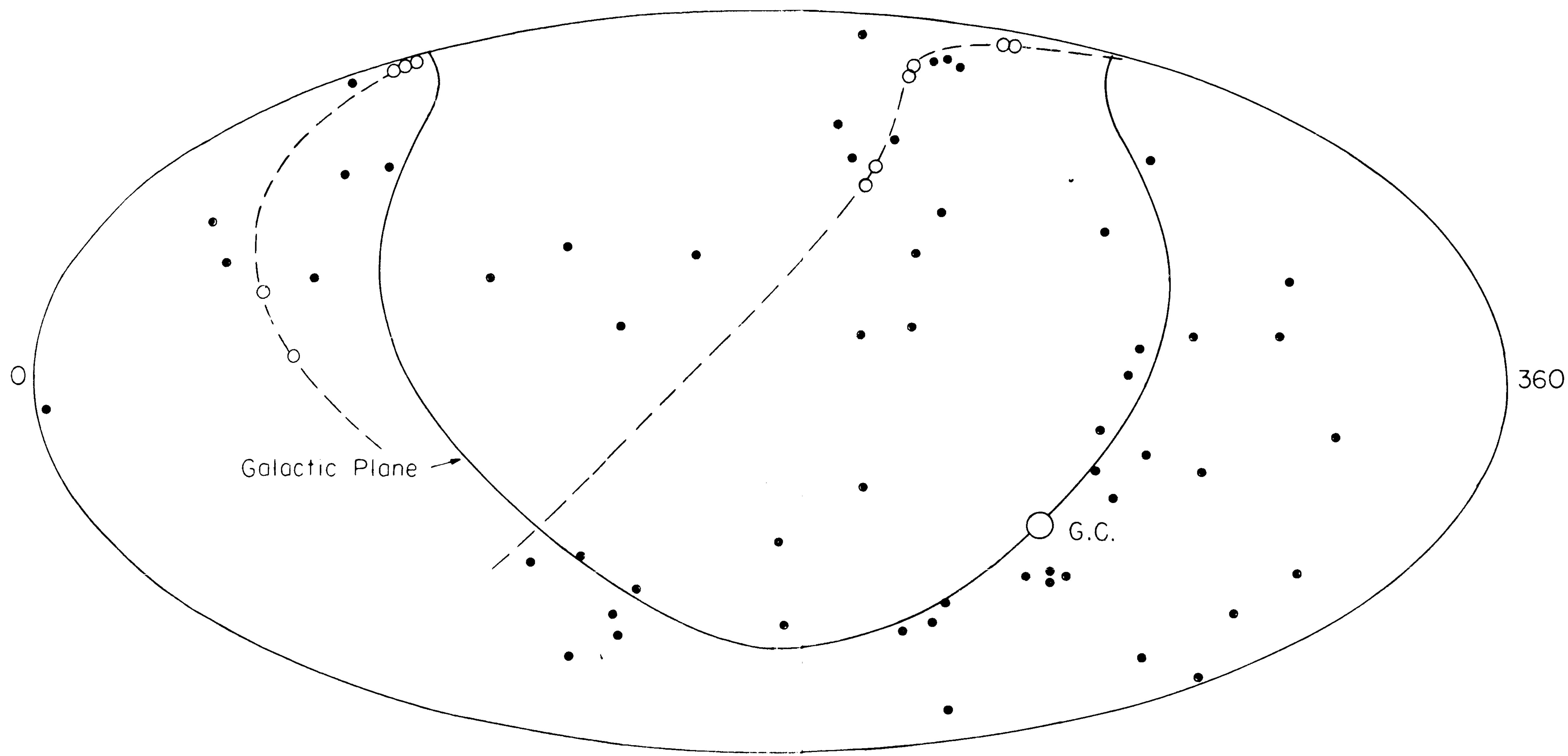

AREAS WITH MORE THAN AVERAGE INTENSITY

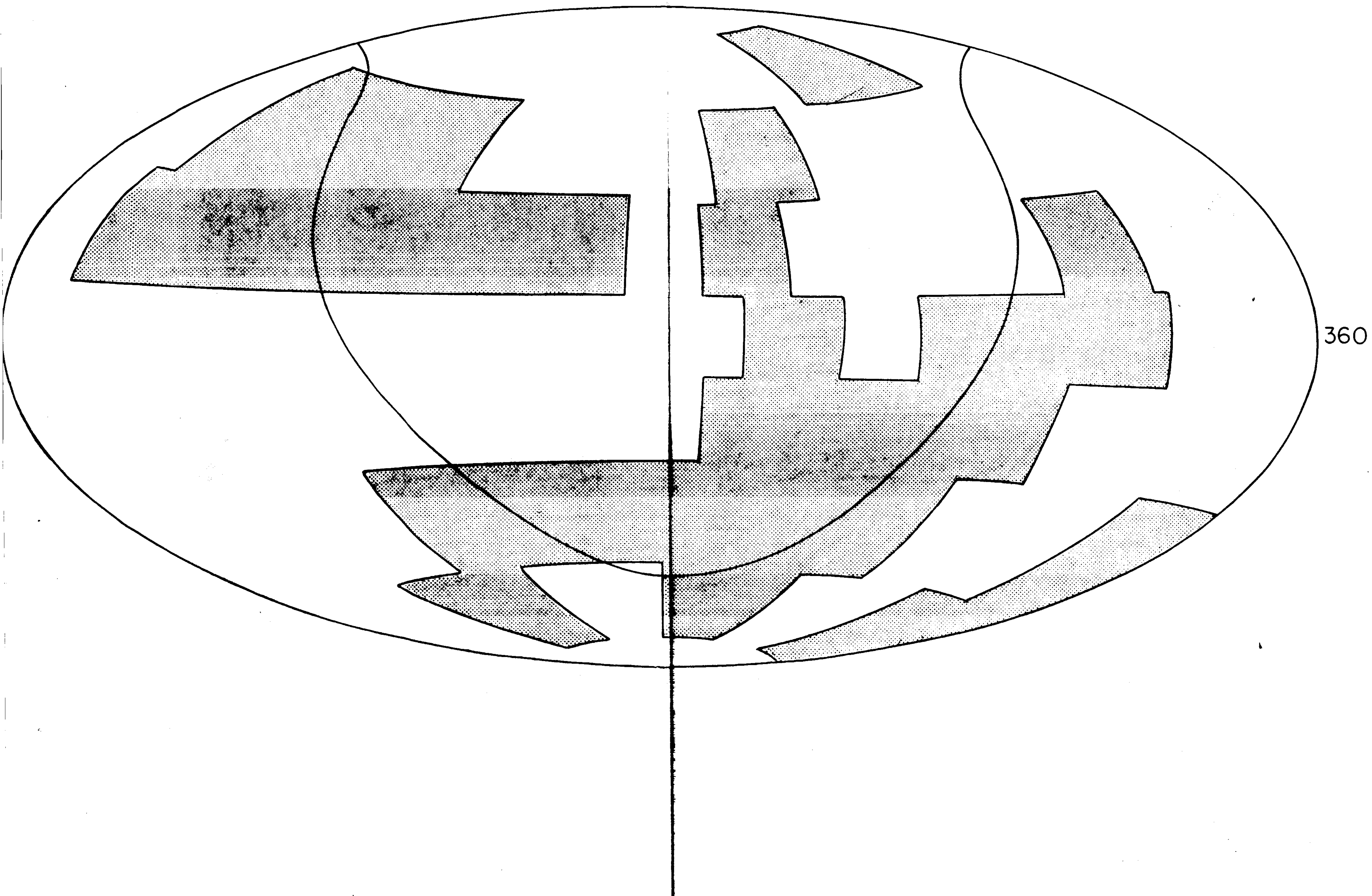

Figure 2. Altitude variation of gamma rays produced by cosmic ray collisions in the earth's atmosphere. The data were taken with a balloon-borne model of the satellite instrument.

Figure 3. Gamma ray events recorded during the early spin phase of the satellite. The time axis is modulo 108 minutes, the orbital period.

Figure 4. Angular distribution of observed gamma ray events.

Figure 5. Pulse height distributions from the high Z sandwich scintillator during calibration, and gamma ray logic periods.

Figure 6. Equal area projection of the celestial sphere showing the celestial coordinates of each detected event. The solid line is plane of the galaxy, and G. C. indicates the galactic center. The dotted line indicates the path of the satellite angular momentum during the early spin phase.

Figure 7. Areas of the celestial sphere in which the detected intensity was at all more than average. The detected distribution is consistent with isotropy.